Seismic geomorphology anomalies within a Pliocene deepwater channel complex in the Taranaki Basin, offshore New Zealand

Julian Chenin[1], Clayton Silver[1], and Heather Bedle[1]

Abstract

The Taranaki Basin, located offshore New Zealand, is a Cretaceous rift basin that has well defined yet complex Miocene deepwater sedimentary systems. We analyze a pronounced anomalous seismic response in a Late Miocene to Early Pliocene deepwater channel within the 2005 Hector 3D survey located in the southern Taranaki Basin. Several seismic attributes were calculated to interpret the extent of these anomalous features. Analogues within both the Iron River reservoir in Albania, Canada and the East Breaks Basin Four, offshore Gulf of Mexico suggest that these anomalous seismic features are most likely channel-body basal scours. Another interpretation suggests that these scours were formed and later filled by mass transport deposits (MTDs) with sediment ponding as suggested from some studies within the Molasse Basin in southern Germany. Alternatively, these scours could also be interpreted as pockmarks resulting from channel abandonment and fluid escape due to compaction. Others describe this process within submarine canyon systems, offshore Equatorial Guinea. However, there is compelling evidence to suggest that these features are most likely channel-body basal scours rather than being related to MTDs or pockmarks. Within all of the interpretations, there is evidence of differential compaction, which is further supported by the reflectors displaying a slight doming immediately above where the scours are located.

Geological feature: Seismic geomorphology anomalies within a Pliocene deepwater channel complex in the Taranaki Basin, offshore New Zealand

Seismic appearance: Asymmetric bowl-shaped geometry with high-amplitude reflectors that are incised into underlying sediment

Alternative interpretations: Pockmarks resulting from channel abandonment and fluid escape due to compaction

Features with similar appearance: Channel scours or pockmarks

Formation: Mount Messenger Formation, Taranaki Basin

Age: Late Miocene to Early Pliocene

Location: Southern Taranaki Basin, New Zealand

Available data: Hector 3D data set, Kiwa-1, and Hector-1 wells

Analysis tools: 3D seismic data, well logs, and seismic attributes

Geologic summary

The Taranaki Basin is a long-lived basin located offshore New Zealand, formed initially by Cretaceous rifting, and it contains world-class Middle Miocene progradational clinoforms and deepwater sedimentary systems. Basin subsidence took place through the Oligocene and Early Miocene as a result of the Pacific Plate subducting below the Australian Plate (Kroeger et al., 2019). Uplift associated with plate subduction and the formation of current tectonic plate boundaries led to a shelf-to-slope progradation of the continental shelf during the Middle Miocene (King and Thrasher, 1996; Vonk and Kamp, 2008; Bull et al., 2019; Strogen et al., 2019). The progradation was modified by fourth-order relative sea-level fluctuations, which resulted in these processes that led to the formation of a deepwater channel complex. These deposits belong to the older Moki (16.7–15.1 Ma), Waiauan (or Sw-sands) (13–11 Ma), Mount Messenger (10.4–8.2 Ma) Formations and the younger Urenui (10.4–8.2 Ma), the Mount Messenger Formation being the interval of interest in this study (Hansen and Kamp, 2002; Rotzien et al., 2014). The Mount Messenger and Urenui Formations were deposited over a period of 2.2 Ma from 10.4 to 8.2 Ma and are best

[1]University of Oklahoma Norman Campus, School of Geosciences, Norman, Oklahoma 73019-0390, USA. E-mail: julian.chenin@ou.edu (corresponding author); clayton.j.silver-1@ou.edu; hbedle@ou.edu.

Manuscript received by the Editor 30 January 2020; revised manuscript received 13 September 2020; published ahead of production 11 November 2020; published online 20 January 2021. This paper appears in *Interpretation*, Vol. 9, No. 1 (February 2021); p. C1–C10, 7 FIGS., 1 TABLE.
http://dx.doi.org/10.1190/INT-2020-0037.1.

developed onshore, in the northeastern region of the Taranaki Basin, where it is approximately 900 m thick (King and Thrasher, 1996; Rotzien et al., 2014). Outcrop studies are mainly onshore and divide the Mount Messenger Formation into two parts: The lower portion of the formation is characterized by thick packages of fine- to very fine-grained sandstone, with some volcaniclastic beds, thick mudstone packages, and mass-transport deposits (MTDs); the upper portion of the formation contains thick- to thin-bedded, sand-rich turbidites and thick packages of muddy turbidites that are thinly bedded (King et al., 1994; King and Thrasher, 1996; Rotzien, 2013; Rotzien et al., 2014). The Upper Mount Messenger Formation has been interpreted as a slope fan with channel, levee, lobe, and overbank environments (King and Thrasher, 1996; King and Browne, 2001; Rotzien et al., 2014). The slope fans were deposited near the base of a prograding continental shelf in bathyal water depths with a significant amount of clastic input (Rotzien et al., 2014). The Mount Messenger Formation is capped by a mudstone-dominated unit in a slope environment with incised channel complexes known as the Urenui Formation (King and Thrasher, 1996; Hansen and Kamp, 2002; Rotzien et al., 2014).

This paper focuses on one deepwater channel among many others, which shows pronounced scour-like morphologies that have not yet been documented within the Upper Mount Messenger Formation in the Hector 3D survey (Figure 1a and 1b; acquired in 2005) located in the southern Taranaki Basin. This Late Miocene to Early Pliocene channel is located within the lower slope to the base of the slope depositional environment (Figure 1a and 1b) (Bull et al., 2019; Strogen et al., 2019). Seismic attributes were calculated and interpreted to map the extent of these scour-like features. Improving the geologic understanding of the scours and possible distribution of associated reservoir-quality sandstones and compartmentalization will have important applications for the exploration and production of hydrocarbons (King and Browne, 2001; Rotzien et al., 2014).

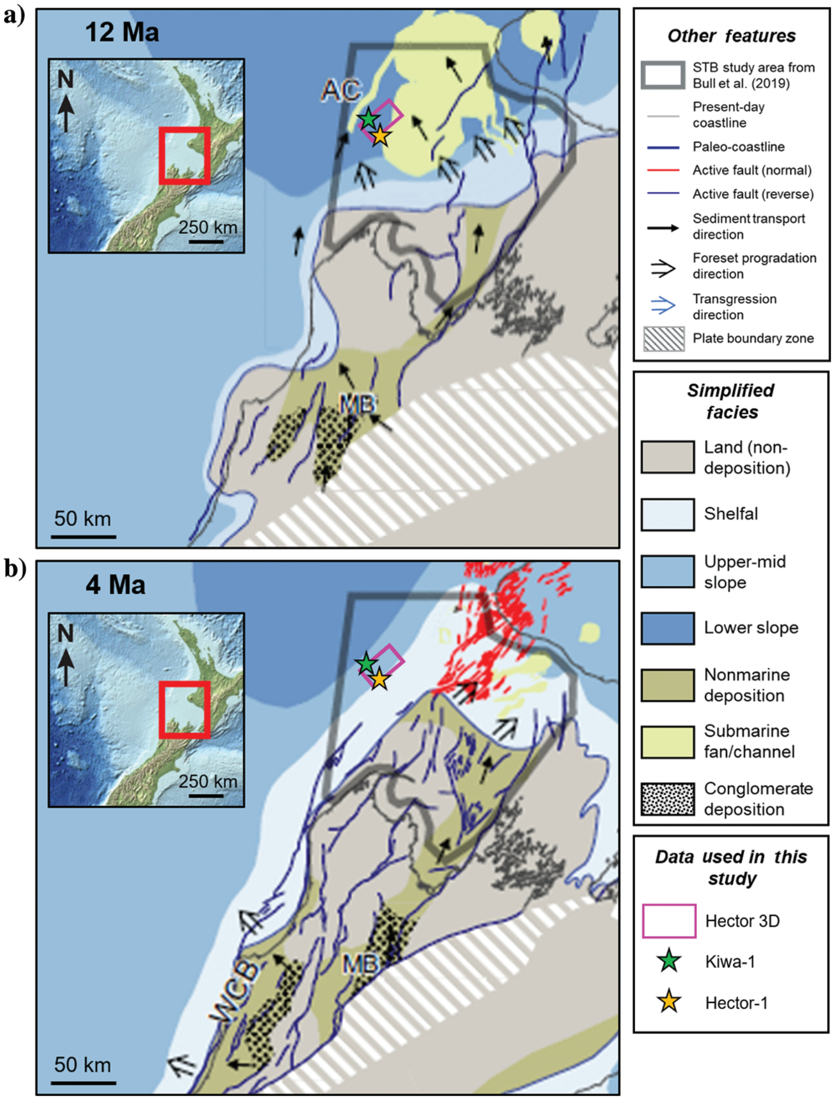

Figure 1. Paleogeographic maps modified from Bull et al. (2019) for (a) the Miocene and (b) the Pliocene of central Zealandia with available data. The Hector 3D data set is shown in magenta, whereas the Kiwa-1 and Hector-1 wells are shown by the green and orange stars, respectively. AC, axial channel; WCB, West Coast Basin; and MB, Murchison Basin (modified from Bull et al., 2019).

Appearance on seismic data

Within the study interval, several channel-like depressions are present within the southwestern portion of the Hector 3D survey (shown by the yellow arrows in Figure 2a). However, one particular channel-like depression has a typical thalweg geometry in cross section but an undulating bottom surface along the dip section, forming amalgamated, isolated depressions (Figure 2a–2d). The channel itself spans the entire length of the survey and is approximately 18 km long by 1 km wide. The sinuosity ratio (SR) was calculated by dividing the length of the channel by the straight-line distance (Posamentier and Kolla, 2003). The channels within this study are straight (SR ~ 1.00) with few channels exhibiting low sinuosity (a max SR of 1.10). These isolated depressions are quite large because they possess a length and width of approximately 500 × 650 m, while being 30 ms deep (roughly 42 m using an average interval velocity of 2850 m/s). The interpreted base of these depressions is a strong seismic reflector, which suggests a high impedance contrast to the underlying sediments, which may reflect a lithologic boundary (Figure 2c and 2d). However, no abrupt change in lithology is observed within the Kiwa-1 gamma-ray log response, which shows mainly a mixture of shale and sand. It is also important to note that the Kiwa-1 did not penetrate the infill of the observed isolated depressions and therefore may not be representative (Figure 2c). Additionally, the acoustic impedance values are lower comparable to the base of the isolated depressions (Figure 2b).

Attribute analysis

Several attributes, such as variance, gray-level cooccurrence matrix (GLCM) average energy, curvature, and spectral decomposition, were generated to further explore the architecture and infill of the anomalous depressions. Variance, curvature, and GLCM average energy were extracted on the interpreted base of the depressions shown in (Figure 3a–3e). Variance, a geometric attribute, was generated to reveal the discontinuities created by the depressions within the channel body. This attribute was also helpful in identifying the edges of the channel in which the depressions were formed (Figure 3b). Curvature is a measure of the bends and breaks of seismic reflectors. A positive curvature represents a positive structure (such as an anticline or channel levees), whereas a negative curvature represents a negative structure (such as a syncline or channel bodies) (Chopra and Marfurt, 2007). The most-positive (k1) and most-negative (k2) curvatures were calculated to better characterize the channel's geometry. These two attributes were helpful for visualizing the channel axes and levees (shown in Figure 3c and 3d). GLCM average energy measures the change in amplitudes and is a statistically calculated, textural attribute (Chopra and Marfurt, 2007). A smooth amplitude variation corresponds to a high GLCM energy value and to a low value if the amplitudes vary abruptly. Low GLCM values are observed where the depressions are occurring because there is an abrupt change in amplitude and it further highlights their geometry (shown in Figure 3e). This amplitude change is further supported by the extracted amplitude value on the interpreted base of the scours (Figure 3a). Spectral decomposition data were generated using the Fourier transform (Peyton et al., 1998), using 13, 37, and 62 Hz (based on the power spectrum in the studied interval), and an RGB color blend was used for visualization (shown in Figure 3f). The tuning thickness of the isolated depression rims is similar within the channel-like incisions, sharing a dominant frequency response of 13 Hz. However, the infills of these isolated depressions are yellow compared to the red color of the rims and the infills of the other channels, showing a dominant frequency response of 25 Hz. The different frequency response suggests that there is some slightly heterogeneous infill compared to the other channels (shown by the black arrows in Figure 3f). The spectral decomposition was also helpful in highlighting the boundaries of the channel and extent of the depressions.

Proposed interpretation

The studied channel is very straight, which is unusual, but it does fit within the setting of very high sedimentation with rapid slope progradation (Baur

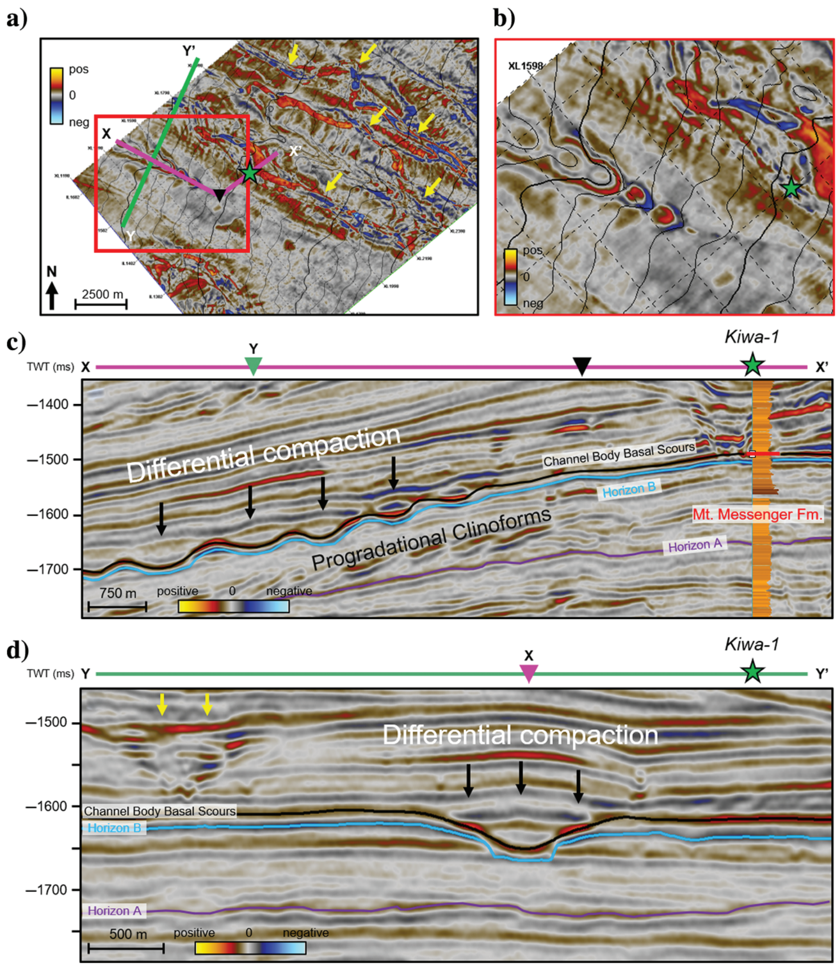

Figure 2. (a) Amplitude extracted onto the interpreted base of the channel-body basal scours highlighting the numerous incised channels (the yellow arrows) within the shown portion of the interval in the southwestern portion of the Hector 3D survey and (b) A magnification of the red box shown in panel (a) to further highlight the anomalous amplitude pattern. Arbitrary lines were taken (c) along the dip and (d) along the strike of the basal scours. The interpreted base of the basal scours is shown by the black horizon in panels (c and d). The black arrows in (c and d) indicate areas of differential compaction. The Kiwa-1 well was tied to the seismic data set, and it revealed that the basal scours are present within the Upper Mount Messenger Formation. The gamma-ray log displayed on the section shows that the interval is composed of a mixture of sand and mud.

et al., 2011; Bull et al., 2019). The undulations at the base of the channel are interpreted as channel scours in the study interval and increase in size basinward (Figure 2a–2d). This increase in size may suggest that the undulations become more erosive downslope as they gain momentum. These scours formed in a deepwater setting most likely resulting from turbulent flows that eroded the base of the channel (Salter, 1993; Gibling, 2006; Snedden, 2013). Scours are formed by the process of turbulent erosion and are part of the erosional processes that form incised river valleys and deepwater canyons (Snedden, 2013). In addition, scours can form within the channel body or at the mouth of the channel (Gibling, 2006; Snedden, 2013). Scours vary significantly within deepwater settings and can appear as isolated or amalgamated erosional features with complex infill (Snedden, 2013). Lithology does not appear to have significant control on the location and size of these scours because there are no changes in acoustic impedance within the underlying sediment that has been eroded away (Figure 2c and 2d). There also appears to be some evidence for differential compaction where the scours are located. This is further supported by the reflectors displaying a slight doming immediately above where the scours are present (shown by the black arrows in Figure 2c and 2d). Additionally, the 25 Hz frequency observation suggests a more heterogeneous infill compared to the lower frequency infill within the other channels (shown by the black arrows in Figure 3f). These observations of differential compaction, high acoustic impedance contrast, and different frequency responses would suggest perhaps a sandier infill.

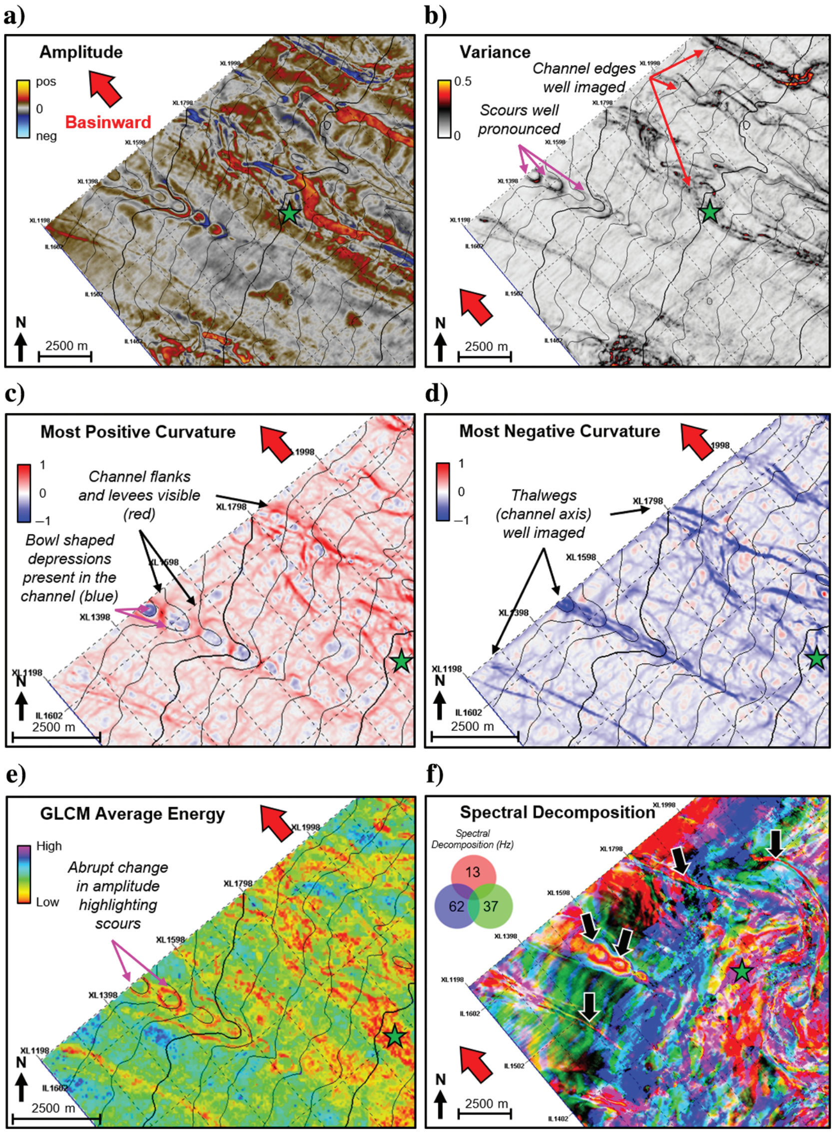

Figure 3. (a) Amplitude, (b) variance, (c) most-positive curvature (k1), (d) most-negative curvature (k2), and (e) GLCM average energy extracted onto the interpreted base of the channel-body basal scours, which is shown in Figure 2a–2d. (f) Spectral decomposition was taken at a time slice of −1628 ms and was generated by blending isofrequency volumes of 13, 37, and 62 Hz. The red arrows point basinward, whereas the green star shows the location of the Kiwa-1 well.

Alternative interpretations

One alternative interpretation is that the scour-like features are actually a result of the topography created by an underlying MTD, where sediment ponding occurred postdeposition (shown by the yellow polygons in Figure 4a–4c). In this alternative interpretation, horizon A highlights the detachment surface upon which the sediment flowed, located roughly 50–100 ms below the interpreted base of the scour-like features (Figure 4c). Within this section, the MTD is characterized by chaotic reflectors. This interpretation suggests that this is not a channel but rather a scar left behind from an underlying MTD. The resulting topography created by these MTDs from their margins and corrugated upper surfaces can capture turbiditic sediment through a process called ponding (Kremer et al., 2018). A study by Beaubouef and Abreu (2006) noted that the channel scours present within the East Breaks Basin Four were also filled as a result of ponding. Examples of sediment ponding within MTD systems have been well studied in Oligocene to lower Miocene strata deposited along the slope, within the Molasse Basin, southern Germany (Figure 4a and 4b). Therefore, the depositional setting is similar to the Mount Messenger Formation, where MTDs have also been observed (King and Thrasher, 1996; Rotzien, 2013; Rotzien et al., 2014). Extensional and compressional faulting of the MTDs can create additional accommodation in which other gravity flows can preferentially pond and deposit (Kremer et al., 2018). This ponding effect is shown on a larger scale in Figure 4a and 4b. This sediment ponding concept is further interpreted on a dip section along the studied channel feature from the Hector 3D data set (Figure 4c).

However, no other MTDs were identified within the Mount Messenger interval of the Hector 3D survey. Yet, several studies note that MTDs are present within the Upper Mount Messenger Formation (King and Thrasher, 1996; Rotzien, 2013; Rotzien et al., 2014). In addition, laterally continuous reflectors are observed above horizon A where the MTD was interpreted when viewing an arbitrary line perpendicular to the dip of the anomalous feature (Figure 2c and 2d and shown by the yellow arrows in Figure 4c). These straight horizons between the interpreted MTD and isolated depressions suggest that there is no relict topography. Furthermore, no progressive deformation is observed downslope. These observations contradict the interpretation of chaotic reflectors, making the MTD interpretation less likely.

Another interpretation builds upon the model proposed by Jobe et al. (2011) where these scours are interpreted as pockmarks resulting from channel abandonment and fluid escape due to compaction (Figure 5). Jobe et al. (2011) describe how circular pockmarks form as a result of canyon abandonment offshore Equatorial Guinea (Figure 5). Erosional, sand-rich, submarine canyon systems dominated the continental margin of Equatorial Guinea during the late Cretaceous and were abandoned during the Paleogene, to be reactivated during the Miocene as a result of tectonic uplift (Jobe et al., 2011). As the canyon is abandoned, erosive fluid escape triggered by sediment compaction creates depressions and adjacent cross ridges form due to sediment deposition, thereby creating intracanyon irregularities (stage 1 in Figure 5) (Jobe et al., 2011). Over time, an alternation of ridges and pockmark depressions occurs within the canyon (stage 2 in Figure 5), until the ridges fill the former canyon morphology and discrete pockmarks are present (stage 3 in Figure 5) (Jobe et al., 2011). There are several channel complexes present within the Upper Mount Messenger Formation with evidence of channel abandonment (Figure 6a–6d). Flattening the sections relative to horizon B (shown in Figure 2c and 2d) showed how the older channel, containing the studied scours (channel 1), was abandoned in favor of a younger channel 2 due to upslope flow capture (shown by the green arrow in Figure 6a–6d).

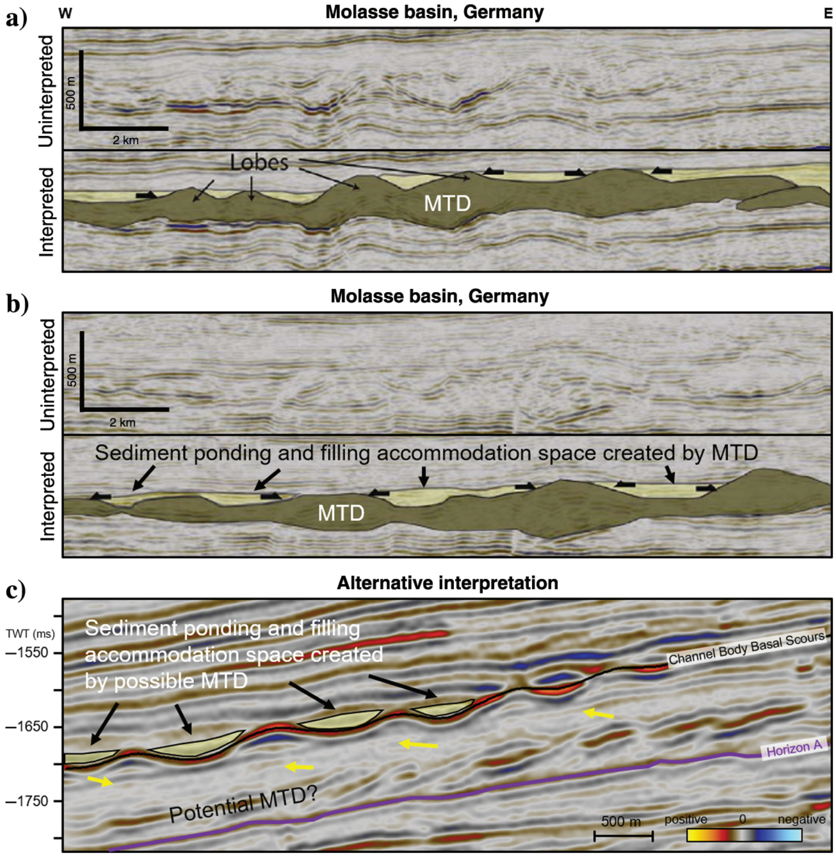

Figure 4. Long-runout MTDs from the Molasse Basin in southern Germany shown in two different vertical amplitude sections (a and b) from Kremer et al. (2018). Other sediment gravity flows are ponding and filling the accommodation space created by the MTD postfailure (modified from Kremer et al., 2018). This is juxtaposed next to (c) the same arbitrary line along dip from Figure 2c and further highlights the possible alternative interpretation. The black horizon highlights the interpreted base of the scours, whereas horizon A highlights the interpreted detachment surface of the MTD. The yellow polygons in (c) highlight the sediment ponding and filling the rugose topography of the MTD, whereas the yellow arrows point to the laterally continuous reflectors observed above horizon A.

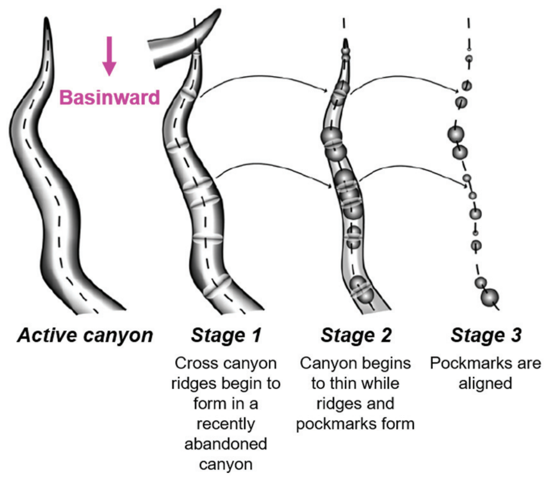

Figure 5. The stages of canyon abandonment from Jobe et al. (2011). The ridges are formed with stage 1 due to fluid escape and eventually form the linear pockmarks observed in stage 3 (modified from Jobe et al., 2011).

Additionally, some of the individual stages for channel abandonment and pockmark formation were discernible within the section from Figure 6a–6d. On the deeper time slices (Figure 6a and 6c), the original channel prior to scouring is shown where some small ridges and pockmarks are beginning to form within the channel body. This is closer to stages 1 and 2 described by Jobe et al. (2011). However, larger pockmarks begin to form in the original channel (channel 1) in the shallower time slices (Figure 6b and 6d). At this point, channel 1 is completely abandoned and is more similar to stage 3 described by Jobe et al. (2011). The dimension of the pockmarks observed in their study is approximately 400 m in diameter while being 50 ms (38 m) deep on average (Jobe et al., 2011). These dimensions are somewhat similar to the scour dimensions observed within the Hector 3D survey (shown in Table 1). Additionally, the scours described by Jobe et al. (2011) were formed in a similar depositional environment to the scours that were formed in the Hector 3D survey.

The alternative pockmark interpretation implies that these possible channel scours could be ambiguous. In this interpretation, the pockmarks resulted from channel abandonment and fluid escape due to differential compaction. However, if these scour-like features are in fact pockmarks, they would need to be related to some deeper structure, which is not evident in the study interval. These pockmarks would need sources for pres-

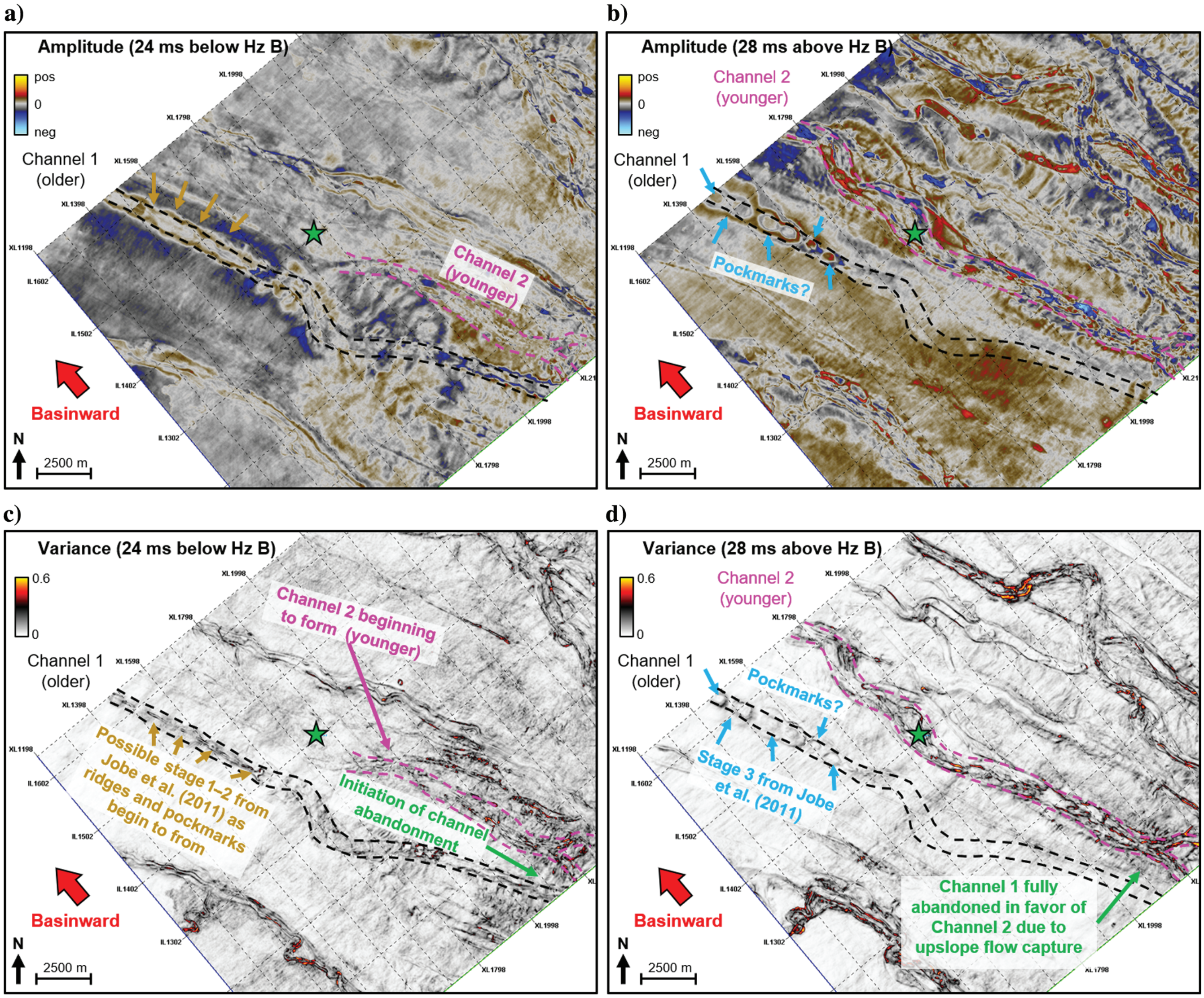

Figure 6. (a and b) Amplitude and (c and d) variance time slices flattened onto horizon B from Figure 2c and 2d highlighting channel abandonment within the Upper Mount Messenger Formation. At 24 ms below horizon B, we see the original channel before the scouring formed. However, as we go up `section (b and d), we see that the channel is abandoned in favor of the younger channel 2. The original outline of channel 1 is overlain on the shallower sections of (b and d). As a result, pockmarks have formed in the abandoned channel 1 coupled with possible fluid escape. The green arrows point to where the channel abandonment occurs. The blue arrows indicate the pockmarks resulting from Jobe et al.'s (2011) process of channel abandonment and fluid escape. The green star marks the location of the Kiwa-1 well.

surized fluids and other indicators that fluids moved through the sediment. This has not been observed within our study interval. Furthermore, although gas-escape structures are commonly observed in the Taranaki Basin, none are observable within the study interval of the Hector 3D survey (Ilg et al., 2012). These considerations further hinder the interpretation because there would need to be pressurized fluids to create the pockmarks (Jobe et al., 2011). Finally, the studied channel is a well-defined structure (Figures 3a–3f and 6a–6d) sharing many similarities with other channels within the study area in terms of dimensions and sinuosity (Figure 6d). It would be highly unlikely for pockmarks to exist in only one channel and not in the nearby channels.

Although several alternative interpretations exist for the undulating morphology at the base of a channel-like body within the Hector 3D survey, there is compelling evidence to suggest that these features are most likely channel-body basal scours rather than a small-scale MTD or pockmarks. The scour interpretation is further supported by characteristic elements from possible analogues within the Iron River Valley in Alberta, Canada and within the East Breaks Basin Four, offshore the Gulf of Mexico.

Possible analogues

Channel-body basal scours are observed in other fluvial and deepwater systems. In fluvial systems, the vertical dimensions of scours are significant in relation to the bank full depth (Keller and Melhorn, 1978; Snedden, 2013). Several studies also observed a scaling relationship between the channel width and the scour-to-scour spacing (Keller and Melhorn, 1978; Thompson, 2002; Snedden, 2013). In deepwater systems, many of the same type of scours seen in fluvial systems are also present (Snedden, 2013). These scours vary from isolated to amalgamated erosional features, with complex sedimentary infills (MacDonald et al., 2011; Snedden, 2013). MacDonald et al. (2011) identify four distinct, deepwater scour morphologies: spoon-shaped, heel-shaped, crescent-shaped, and oval-shaped. These deepwater scours ranged from 40 to 3170 m wide and 8 to 48 m deep (MacDonald et al., 2011). The sizes of the scours are primarily controlled by their location, the flow regime, and gradient changes (Carvajal et al., 2017). Salter (1993) notes that channel-base scours are common near the outer bends of rivers. Carvajal et al. (2017) observe larger scours within the overbank area with high gradients and high flow regimes (Carvajal et al., 2017).

One example of fluvial scours is located in Alberta, Canada, where the Cretaceous Iron River fluvial reservoir exhibits similar scouring features to those observed in the study interval (Figure 7a). The scours present within the Iron River Valley are shown on depth maps of selected channels where the basinward direction is northward and colder colors highlight deeper areas (Snedden, 2013). These scours are approximately

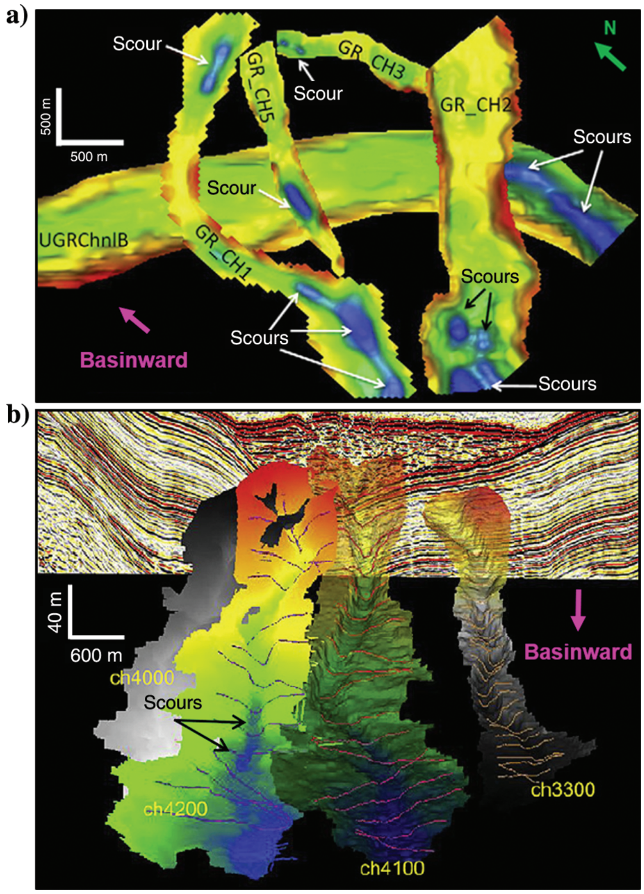

Figure 7. (a) Scours were similarly identified from Snedden (2013) within the Iron River valley and (b) within the East Breaks Basin Four. The scours shown in (a and b) were taken on a depth map of selected valleys and channels where the colder colors highlight deeper areas (modified from Snedden, 2013).

Table 1. Channel sinuosity and average geometries of the discussed channel scours and pockmarks.

Study	Avg. width (m)	Avg. length (m)	Avg. thickness (m)	Area (km^2)	Channel sinuosity
Hector 3D	500	650	42	0.325	1.00–1.10
Jobe et al., 2011	400	400	38	0.160	1.07–1.14
Snedden (2013) Iron River Valley	200	300	15	0.060	1.02–1.09
Snedden (2013) East Breaks Basin Four	220	500	15	0.110	1.10–1.17

200 m wide, 300 m long, and they are roughly 15 m deep. Although these scours are smaller in comparison to the scour dimensions observed in the Hector 3D survey, both scours appear to have the same geometries (asymmetrical and bowl-shaped depressions) (shown in Table 1). An example of deepwater scouring has been observed in the East Breaks Basin Four, offshore Gulf of Mexico shown in Figure 7b (Snedden, 2013). The East Breaks Basin Four is a late Pleistocene, deepwater fan belonging to the Brazos-Trinity slope system, which contains several channel-bodies and lobes located within the intraslope (Beaubouef and Abreu, 2006; Snedden, 2013). The East Breaks Basin Four scours are approximately 15 m deep while being roughly 220 m wide and 500 m long (Snedden, 2013). These scour dimensions are also smaller when compared to the dimensions observed in the Hector 3D data set (shown in Table 1), yet both scours exhibit similar shapes.

Although fluvial and deepwater scours share similar dimensions and geometries, the channel elements and scours of the East Breaks Basin serve as a better analogue for our study because they are situated within a deepwater system (Hansen and Kamp, 2002; Rotzien et al., 2014; Bull et al., 2019; Strogen et al., 2019). The Hector 3D scours may be larger than both analogues due to differences in location along the channel, gradient, and flow regime (Carvajal et al., 2017). Additionally, the dimensions of our interpreted scours also fit within the range of deepwater scours described by MacDonald et al. (2011).

Conclusion

This study documents an undulating bottom profile of a deepwater channel-like body, outlining isolated depressions in the Hector 3D survey, Taranaki Basin (New Zealand), and it considered several possible interpretations (turbiditic scours, ponding on MTD relict bathymetry, and pockmark origin). Based on the lack of relict topography supported by the straight horizons found between the scours and previously interpreted MTD as well as the lack of no clear, deep fluid source for the pockmarks, the isolated depressions likely reflect erosive scours resulting from turbiditic flows. There is compelling evidence to suggest that these features are most likely channel-body basal scours rather than being related to MTDs or pockmarks. Furthermore, the geometry of these scours is similar to the dimensions of the presented analogues as well as the findings from MacDonald et al. (2011) (shown in Table 1). The differences in scour geometries could be due to differences in their location, gradient, and flow regime (Carvajal et al., 2017). The authors encourage readers to contribute their interpretations and to hopefully stimulate an open discussion among other scientists.

Acknowledgments

We would like to thank New Zealand Petroleum and Minerals for publicly providing the Hector 3D data set and well data. We would also like to thank AASPI for providing the software used to generate various attributes, and we thank Schlumberger for providing the Petrel licenses to the University of Oklahoma (OU). An additional special thank you goes to the OU SDA student researchers for their input on this project. Finally, the authors would like to thank the editors, the associate editor F. Smit, two anonymous reviewers, R. Fongngern, and C. Olariu for their recommendations and constructive criticism that greatly improved this paper.

Data and materials availability

Data associated with this research are available and can be accessed via the following URL: https://data.nzpam.govt.nz/GOLD/system/mainframe.asp.

References

Baur, J. R., P. R. King, T. Stern, and B. Leitner, 2011, Development and seismic geomorphology of a Miocene slope channel megasystem, Offshore Taranaki Basin, New Zealand, *in* L. Wood, T. Simo, and N. Rosen, eds., Seismic imaging of depositional and geomorphic systems: SEPM Foundation, Gulf Coast Section, 30th Annual Research Conference Proceedings, 618–649.

Beaubouef, R. T., and V. Abreu, 2006, Basin 4 of the Brazos-Trinity slope system: Anatomy of the terminal portion of an intra-slope lowstand systems tract: Gulf Coast Association of Geological Societies Transactions, **56**, 39–49.

Bull, S., A. Nicol, D. P. Strogen, K. Kroeger, and H. Seebeck, 2019, Tectonic controls on Miocene sedimentation in the Southern Taranaki Basin and implications for New Zealand plate boundary deformation: Basin Research, **31**, 253–273, doi: 10.1111/bre.12319.

Carvajal, C., C. K. Paull, D. W. Caress, A. Fildani, E. Lundsten, K. Anderson, K. L. Maier, M. McGann, R. Gwiazda, and J. C. Herguera, 2017, Unraveling the channel–lobe transition zone with high-resolution AUV bathymetry: Navy Fan, offshore Baja California, Mexico: Journal of Sedimentary Research, **87**, 1049–1059, doi: 10.2110/jsr.2017.58.

Chopra, S., and K. Marfurt, 2007, Curvature attribute applications to 3D surface seismic data: The Leading Edge, **26**, 404–414, doi: 10.1190/1.2723201.

Gibling, M. R., 2006, Width and thickness of fluvial channel bodies and valley fills in the geological record: A literature compilation and classification: Journal of Sedimentary Research, **76**, 731–770, doi: 10.2110/jsr.2006.060.

Hansen, R. J., and P. J. J. Kamp, 2002, Evolution of the Giant Foresets Formation, northern Taranaki Basin, New Zealand: New Zealand Petroleum Conference Proceedings, 419–449.

Ilg, B. R., S. Hemmings-Sykes, A. Nicol, J. Baur, M. Fohrmann, R. Funnell, and M. Milner, 2012, Normal faults and gas migration in an active plate boundary, southern Taranaki Basin, offshore New Zealand: AAPG Bulletin, **96**, 1733–1756, doi: 10.1306/02011211088.

Jobe, Z. R., D. R. Lowe, and S. J. Uchytil, 2011, Two fundamentally different types of submarine canyons along the continental margin of Equatorial Guinea: Marine and Petroleum Geology, **28**, 843–860, doi: 10.1016/j.marpetgeo.2010.07.012.

Keller, E. A., and W. N. Melhorn, 1978, Rhythmic spacing and origin of pools and riffles: Geological Society of America Bulletin, **89**, 723–730, doi: 10.1130/0016-7606(1978)89<723:RSAOOP>2.0.CO;2.

King, P. R., and G. H. Browne, 2001, Miocene turbidite reservoir systems in the Taranaki Basin, New Zealand: Established plays and analogues for deep-water exploration: PESA Eastern Australasian Basins Symposium.

King, P. R., G. H. Browne, and R. M. Slatt, 1994, Sequence architecture of exposed late Miocene basin floor fan and channel-levee complexes (Mount Messenger formation), Taranaki Basin, New Zealand, *in* P. Weimer, A. H. Bouma, and B. Perkins, eds., Submarine Fans and Turbidite Systems: Sequence Stratigraphy, Reservoir Architecture and Production Characteristics, Gulf Coast and International, Proceedings Gulf Coast Section, Society of Economic Paleontologists and Mineralogists Foundation 15th Annual Research Conference, 177–192.

King, P. R., and G. P. Thrasher, 1996, Cretaceous Cenozoic geology and petroleum systems of the Taranaki Basin, New Zealand: Institute of Geological & Nuclear Sciences, **2**.

Kremer, C. H., T. McHargue, L. Scheucher, and S. Graham, 2018, Transversely-sourced mass-transport deposits and stratigraphic evolution of a foreland submarine channel system: Deep-water tertiary strata of the Austrian Molasse Basin: Marine and Petroleum Geology, **92**, 1–19, doi: 10.1016/j.marpetgeo.2018.01.035.

Kroeger, K. F., G. P. Thrasher, and M. Sarma, 2019, The evolution of a Middle Miocene deep-water sedimentary system in northwestern New Zealand (Taranaki Basin): Depositional controls and mechanisms: Marine and Petroleum Geology, **101**, 355–372, doi: 10.1016/j.marpetgeo.2018.11.052.

MacDonald, H. A., R. B. Wynn, V. A. I. Huvenne, J. Peakall, D. G. Masson, P. E. Weaver, and S. D. McPhail, 2011, New insights into the morphology, fill, and remarkable longevity (>0.2 m.y.) of modern deep-water erosional scours along the northeast Atlantic margin: Geosphere, **7**, 845–867, doi: 10.1130/GES00611.1.

Peyton, L., R. Bottjer, and G. Partyka, 1998, Interpretation of incised valleys using new 3-D seismic techniques: A case history using spectral decomposition and coherency: The Leading Edge, **17**, 1294–1298, doi: 10.1190/1.1438127.

Posamentier, H. W., and V. Kolla, 2003, Seismic geomorphology and stratigraphy of depositional elements in deep-water settings: Journal of Sedimentary Research, **73**, 367–388, doi: 10.1306/111302730367.

Rotzien, J. R., 2013, Processes of sedimentation, stratigraphic architecture, and provenance of deep-water depositional systems: Examples from the Upper Miocene Upper Mount Messenger Formation, Taranaki Basin, New Zealand and Pliocene Repetto and Pico Formations, Ventura Basin, California: Unpublished Ph.D. thesis, Stanford University, 218.

Rotzien, J. R., D. R. Lowe, P. R. King, and G. H. Browne, 2014, Stratigraphic architecture and evolution of a deep-water slope channel-levee and overbank apron: The Upper Miocene Upper Mount Messenger Formation, Taranaki Basin: Marine and Petroleum Geology, **52**, 22–41, doi: 10.1016/j.marpetgeo.2014.01.006.

Salter, T., 1993, Fluvial scour and incision: Models for their influence on the development of realistic reservoir geometries: Geological Society, London, Special Publications, **73**, 33–51, doi: 10.1144/GSL.SP.1993.073.01.04.

Snedden, J. W., 2013, Channel-body basal scours: Observations from 3D seismic and importance for subsurface reservoir connectivity: Marine and Petroleum Geology, **39**, 150–163, doi: 10.1016/j.marpetgeo.2012.08.013.

Strogen, D. P., K. E. Higgs, A. G. Griffin, and H. E. G. Morgans, 2019, Late Eocene–Early Miocene facies and stratigraphic development, Taranaki Basin, New Zealand: The transition to plate boundary tectonics during regional transgression: Geological Magazine, **156**, 1751–1770, doi: 10.1017/S0016756818000997.

Thompson, D. M., 2002, Geometric adjustment of pools to changes in slope and discharge: A flume experiment: Geomorphology, **46**, 257–265, doi: 10.1016/S0169-555X(02)00077-6.

Vonk, A. J., and P. J. J. Kamp, 2008, The Late Miocene Southern and Central Taranaki inversion phase (SCTIP) and related sequence stratigraphy and paleogeography: New Zealand Petroleum Conference Proceedings, 1–18.

Julian Chenin received a B.S. (2018) with university honors in geology from the University of Houston and an M.S. (2020) in geophysics from OU. He has worked in various exploration, development, and research roles as an associate geoscientist at Bluware and most recently within the Permian Basin and Gulf of Mexico as a two-time geophysics intern at Occidental Oil and Gas. His research interests include machine learning for seismic interpretation and characterization. In his free time, he is active with several organizations and serves on the Young Professionals Organizing Committee for GEO2020 and on the AAPG Ad Hoc Sustainable Development Committee. He is a member of AAPG, SEG, SPE, the Houston Geological Society, the Geophysical Society of Houston, and the Geophysical Society of Oklahoma City. When he is not working, he is usually hiking and appreciating the outdoors with his friends.

Clayton Silver received a B.S (2019) in geophysics from OU, and he is currently a master's student there advised by H. Bedle. During his undergraduate years, he worked on a seismic acquisition crew for Dawson Geophysical. He gained experience operating vibroseis trucks and jugging

geophones. Following that, he worked a summer internship with Sigma Cubed as a microseismic processor. He has been a graduate research assistant at OU since 2019. His primary research interests integrate sequence stratigraphy, machine learning, attribute analyses, and seismic geomorphology.

Heather Bedle received a B.S. (1999) in physics from Wake Forest University and then worked as a systems engineer in the defense industry. She later received an M.S. (2005) and a Ph.D. (2008) from Northwestern University. After nine years of working with Chevron, she instructed at the University of Houston for two years, and she has been an assistant professor at OU since 2018. Her primary research interests merge seismic interpretation, rock physics, machine learning, and attribute analysis.